# Assessing the accuracy of hybrid functionals in the determination of defect levels: Application to the As antisite in GaAs

Hannu-Pekka Komsa and Alfredo Pasquarello

*Chaire de Simulation à l'Echelle Atomique (CSEA), Ecole Polytechnique Fédérale de Lausanne (EPFL), CH-1015 Lausanne, Switzerland*

(Received 4 April 2011; revised manuscript received 10 June 2011; published 11 August 2011)

The accuracy of nonscreened and screened hybrid functionals for the calculation of defect levels within the band gap is assessed for the As antisite in GaAs, the nature of which is well characterized experimentally. A set of functionals differing by the fraction of nonlocal Fock exchange or by the screening length are examined. The $+2/+1$ and the $+1/0$ charge transition levels as determined with any of the considered functionals line up when referred to the average electrostatic potential, with a defect-level separation in fair agreement with the experimental value. When the band gap is well reproduced, the calculated defect levels are found within 0.2 eV of the experimental levels. The use of the theoretical rather than the experimental lattice constant for the bulk host is found to affect the defect levels by less than 0.1 eV.

DOI: 10.1103/PhysRevB.84.075207 PACS number(s): 71.15.−m, 71.55.Eq

## I. INTRODUCTION

For the calculation of defect levels within the density functional theory (DFT) framework, two main problems persist: the band-gap error inherent in the use of semilocal functionals and the finite-size effects associated with the long-range nature of the Coulomb interactions for charged defects. Furthermore, it is not clear to what extent current functionals accurately describe the combination of defect and bulk systems, due to the concurrent occurrence of localized and delocalized electronic states.[1–3] Such an assessment is hindered by the difficulty of identifying defects possessing a solid experimental characterization as far as both their electronic and structural properties are concerned.

Hybrid functionals generally lead to an improvement over semilocal functionals for both molecules and extended systems. In particular, due to the considerably improved band gap, hybrid functionals were naturally also applied in defect calculations.[4] The use of different hybrid functionals has been found to lead to close defect levels when referred to the average electrostatic potential of the host material, while the band edges undergo noticeable shifts.[1,5] However, theoretical investigations which carefully benchmark calculated results with respect to reliable experimental data have remained rare. For instance, Deák *et al.* examined the performance of a screened hybrid functional[6] applied to a set of defects in different host materials, obtaining very promising results.[7] The comparison with experiment was facilitated because the adopted functional gave very accurate band gaps and lattice constants for the host materials. However, for a generic host material, the applied hybrid functional does not always yield a band gap matching the experimental one. A common practice consists in adjusting the fraction of Fock exchange in the hybrid functional,[2,5] but the accuracy of the defect levels determined according to this procedure remains to be assessed.

For benchmarking purposes, we here focus on the As antisite defect in GaAs, also known as the EL2 defect. Extensive studies, both experimental and theoretical, have provided an accurate account of the properties of this defect, such as its symmetry, charge states, behavior upon optical bleaching, and thermal recovery.[8,9] In particular, its charge transition levels have been accurately and consistently determined by electron paramagnetic resonance,[10] deep-level transient spectroscopy,[11] photocapacitance spectroscopy,[11,12] and scanning tunneling spectroscopy.[13] The energy levels of the As antisite defect could also be related to the pinning levels at GaAs surfaces upon metallization or oxidation.[14,15] Density functional studies were instrumental for identifying the nature of the EL2 defect.[16–21] However, a stringent comparison between experimental and theoretical defect levels is still lacking because of the band-gap underestimation problem.

In this paper, we assess the accuracy of the defect levels of the As antisite in GaAs calculated with various hybrid density functionals with respect to reliable experimental data. In particular, we compare calculated and measured defect levels for both screened and nonscreened hybrid density functionals, in which the fraction of Fock exchange has been adjusted to match the experimental band gap of the host material. Furthermore, we quantify the importance of performing structural optimization of the defect and of the host material consistent with the adopted hybrid functional.

The paper is organized as follows. In Sec. II, we describe our theoretical approach based on hybrid functionals. In particular, we discuss the role of $3d$ electrons, spin-orbit coupling, long-range structural relaxation, and finite-size effects. The results of our calculations are given in Sec. III, where they are compared to experiment. In Sec. IV, the achieved accuracy is discussed in light of the overall accuracy expected for hybrid functional calculations and the conclusions are drawn.

## II. METHODS

We consider the following set of exchange-correlation functionals: the semilocal Perdew-Burke-Ernzerhof (PBE),[22] the nonscreened PBE hybrid (PBE0),[23] and the screened Heyd-Scuseria-Ernzerhof (HSE) hybrid.[6] The default value of the fraction $\alpha$ of Fock exchange in the PBE0 and HSE functionals is 0.25. However, for both hybrid functionals, we also consider variants tPBE0 and tHSE in which $\alpha$ is tuned to reproduce the experimental band gap. The calculations in this work are carried out with plane-wave basis sets. We use normconserving PBE pseudopotentials for both Ga and As in

 

all calculations.[24] The Ga 3*d* electrons are generally treated as core states and an energy cutoff of 30 Ry is found to yield converged results. When the Ga 3*d* electrons are included among the valence electrons, it is necessary to raise the energy cutoff to 80 Ry. The exchange potential is treated as described in Refs. 25 and 26. We use the code QUANTUM-ESPRESSO,[27] in which we implemented the HSE functional.[5]

GaAs exhibits a fairly large spin-orbit splitting of the valence-band maximum. When spin-orbit effects are explicitly considered at the PBE level,[28] we find a splitting of ∼0.30 eV at the Γ point, to be compared with the experimental value of 0.34 eV.[29] The explicit treatment of Ga 3*d* electrons does not affect the spin-orbit splitting. Similarly, spin-orbit splittings are found to remain unaffected at the hybrid functional level.[30] Hence, in the calculations of this paper, the spin-orbit coupling is generally not considered explicitly, but its effect is accounted for by an *a posteriori* correction of the valence-band edge. More precisely, the valence-band edge is raised by 0.1 eV with respect to its position in a bulk calculation without spin-orbit coupling. This correction is included in all the results reported in this paper. In particular, in the case of tuned hybrid functionals, the fraction $\alpha$ is chosen to produce a band gap of 1.62 eV, in order to achieve the experimental band gap of 1.52 eV after an upward shift of the valence-band edge by 0.1 eV due to the spin-orbit splitting.

The band gaps and lattice constants of GaAs as obtained with the various functionals are collected in Table I. These calculations are performed in the primitive cell with a 12 × 12 × 12 $k$-point mesh. The band gaps vary quite significantly among the hybrid functionals. In contrast, the theoretical lattice constants are within 0.02 Å, overestimating the experimental value by 0.03–0.05 Å. We note that for the two hybrid functional schemes the band gap obtained at the theoretical lattice constant is systematically lower than that achieved at the experimental lattice constant. The explicit treatment of Ga 3*d* electrons generally results in a reduction of the band gap by ∼0.2 eV. Furthermore, as far as their effect on the lattice constant is concerned, a slight deterioration of the agreement with experiment is observed at the PBE level, but this effect turns out to be negligible at the HSE level.

TABLE I. Band gaps of GaAs obtained with various (hybrid) functionals for lattice constant ($a_0$) fixed at the experimental value or determined consistently within the adopted theoretical scheme. The fraction of Fock exchange $\alpha$ is indicated. For the cases denoted PBE(Ga3*d*) and HSE(Ga3*d*), the Ga 3*d* electrons are explicitly included among the valence states. Experimental data are from Ref. 29.

| | Experimental $a_0$ | | | Theoretical $a_0$ | | |
|---|---|---|---|---|---|---|
| | $\alpha$ | $a_0$ (Å) | $E_g$ (eV) | $\alpha$ | $a_0$ (Å) | $E_g$ (eV) |
| PBE | | 5.65 | 0.57 | | 5.75 | 0.17 |
| PBE (Ga3*d*) | | 5.65 | 0.41 | | 5.79 | 0.00 |
| HSE | 0.25 | 5.65 | 1.24 | 0.25 | 5.70 | 1.10 |
| HSE (Ga3*d*) | 0.25 | 5.65 | 1.05 | 0.25 | 5.69 | 0.88 |
| PBE0 | 0.25 | 5.65 | 1.83 | 0.25 | 5.70 | 1.59 |
| tHSE | 0.35 | 5.65 | 1.53 | 0.395 | 5.68 | 1.52 |
| tPBE0 | 0.19 | 5.65 | 1.52 | 0.235 | 5.70 | 1.52 |
| Expt. | | 5.65 | 1.52 | | 5.65 | 1.52 |

To compare with experiment,[10,11] we focus on charge transition levels

$$\mu_{q/q'} = \frac{\left(E^{q'}_{\rm tot} - E^{q}_{\rm tot}\right)}{q - q'} - \varepsilon_v - \Delta V, \quad (1)$$

where $E^q_{\rm tot}$ denotes the total energy for a defect in the charge state $q$, $\varepsilon_v$ is the valence-band maximum as obtained in a separate bulk calculation, and $\Delta V$ is a potential alignment term determined for the neutral defect.

The defect calculations are carried out in 216-atom supercells with 2 × 2 × 2 $k$-point sampling. The $k$-point grid is displaced off the Γ point, thus allowing us to correctly occupy the defect levels even when the band gap is underestimated. On the basis of calculations with dense $k$-point samplings at the PBE level, we estimate that the 2 × 2 × 2 mesh gives total energies converged within 1 mRy and expect higher accuracy for total energy differences.

Structural relaxations in 216-atom supercells at the hybrid functional level are computationally expensive. Therefore, we accounted for the structural relaxations using the following embedding scheme. We first relax the defect structure in a 64-atom supercell with a 2 × 2 × 2 $k$-point sampling, and then embed the obtained structure in the 216-atom supercell without allowing for additional relaxation. We estimate errors on the defect levels resulting from the embedding procedure at the PBE level. When all the atoms of the 216-atom supercell are fully relaxed, the defect levels are found to lie lower by only 15 meV.

For correcting the finite-size supercell errors, we use the method proposed by Freysoldt *et al.*[31] We use a model charge consisting of a single Gaussian and checked that the long-range potential of the model charge well matches that from the supercell calculations. We illustrate the accuracy of this correction scheme within the PBE by considering supercells of increasing size. The defect is modeled with 64-atom, 216-atom, 512-atom, and 1000-atom supercells. We use a 3 × 3 × 3 $k$-point grid in the 64-atom supercell calculation and 2 × 2 × 2 $k$-point grids for the 216-, 512-, and 1000-atom supercells. The uncorrected and corrected PBE results are shown as a function of the supercell size in Fig. 1. We obtain an estimate of 20 meV for the residual error associated to this correction scheme by comparing the corrected formation energies to their extrapolated values (Fig. 1).

To conclude this section, we analyze to what extent the charge transition levels are affected by the approximations adopted in our scheme. To examine the effect associated to the explicit treatment of Ga 3*d* electrons, we calculate the defect levels at the PBE level using a 64-atom supercell at the experimental lattice constant with and without Ga 3*d* electrons included among the valence states (Table II). When the Ga 3*d* electrons are among the valence states, the separation between the defect levels remains unaffected. However, as a consequence of the reduction of the band gap, the defect levels are found to be lower in the band gap by 0.07 eV. When the fraction of nonlocal Fock exchange is adjusted to give the experimental band gap, we can assume that the defect levels remain unchanged with respect to the average electrostatic potential (see below).[1] By considering the shift of the band edges, we then estimate that the explicit treatment of Ga 3*d*

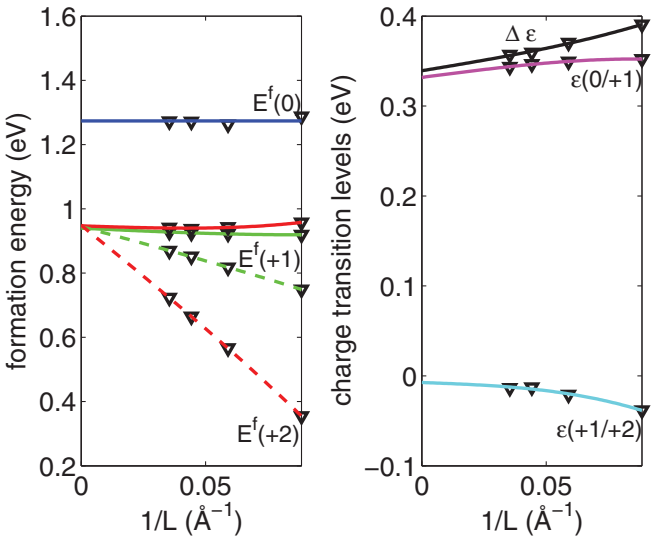


FIG. 1. (Color online) Formation energy (left-hand side) and charge transition levels (right-hand side) calculated at the PBE level as a function of the inverse side $(1/L)$ of the supercell. The extrapolated values are obtained from a regression to $a + b/L + c/L^3$ of the results without (dashed lines) and with (solid lines) finite-size corrections. In the formation energy, the chemical potential of As corresponds to the $As_4$ molecule and that of Ga then results from the equilibrium condition for GaAs.

electrons in tHSE would lead to defect levels higher in the band gap by 0.07 eV.

To analyze the effect of an explicit treatment of the spin-orbit coupling on the defect levels, we carried out PBE calculations using the same 64-atom model. From Table II, we see that the spin-orbit coupling effects are very accurately accounted for by the upward shift of the valence-band maximum by 0.1 eV, yielding errors of at most 30 meV.

In summary, this analysis allows us to estimate the errors involved in our calculation scheme. The most significant error results from the implicit treatment of Ga $3d$ electrons: $-70$ meV in the PBE and $+70$ meV in tHSE. Finite-size supercell corrections give an additional uncertainty of 20 meV. Errors associated to an incomplete structural relaxation ($-15$ meV) and to an incomplete $k$-point sampling ($-10$ meV) are much smaller. Thus, we estimate that our computational approach gives charge transition levels within an overall accuracy of 0.1 eV. In tHSE, the error associated to the Ga $3d$ electrons is partially compensated by the errors resulting from structural relaxation and $k$-point sampling, leading to an even higher accuracy.

TABLE II. Charge transition levels given with respect to the valence-band maximum when the Ga $3d$ electrons or the spin-orbit coupling (SOC) is explicitly accounted for, compared to a reference PBE calculation in which these effects are treated implicitly. The results correspond to a 64-atom supercell at the experimental lattice constant. The respective band gaps ($E_g$) are given. Energies are given in eV.

| | $E_g$ | $+2/+1$ | $+1/0$ |
|---|---|---|---|
| PBE | 0.57 | $-0.04$ | 0.37 |
| PBE with Ga $3d$ | 0.41 | $-0.10$ | 0.30 |
| PBE with SOC | 0.60 | $-0.05$ | 0.37 |

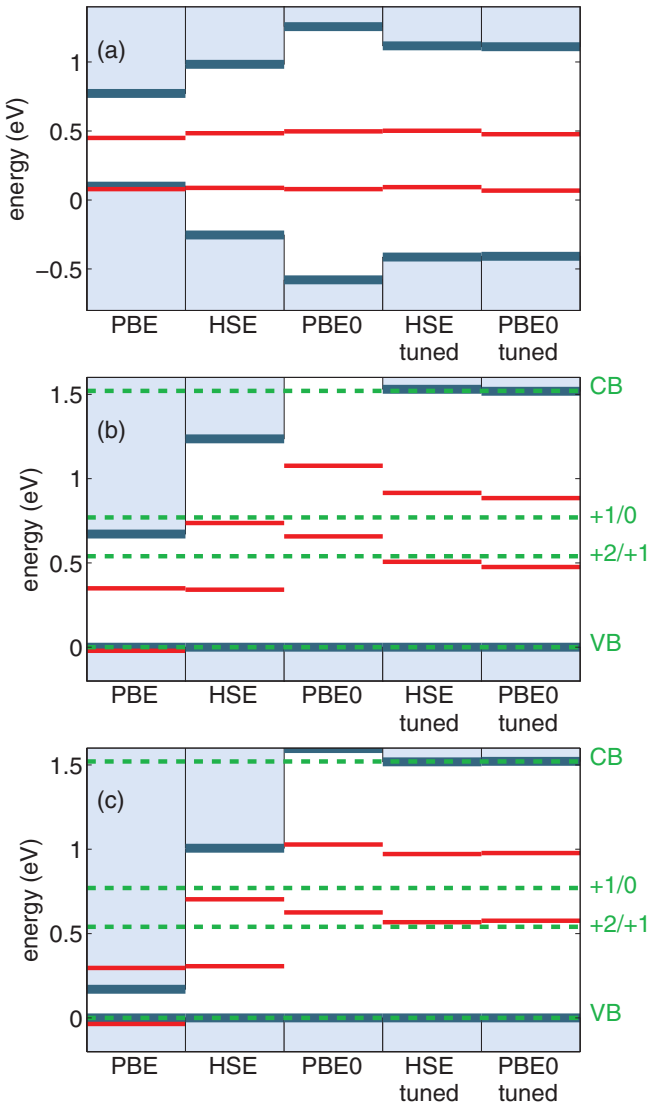


FIG. 2. (Color online) Charge transition levels $+2/+1$ and $+1/0$ of the As antisite in GaAs calculated with various functionals, aligned with respect to (a) the average electrostatic potential and to (b),(c) the valence-band maximum. In (a) and (b), the defect structure is relaxed at the HSE level and the experimental lattice constant is adopted. In (c), the lattice constant and the defect structure are consistently determined with the adopted functional. Experimental levels (dashed) are from Ref. 11. The numerical values used in (b) and (c) are given in Table III.

## III. DEFECT LEVELS OF THE As ANTISITE IN GaAs

In order to focus on electronic effects, we first determine the defect levels for various functionals while keeping a fixed defect geometry. For this, we use a lattice constant fixed at the experimental value and structural relaxations carried out with HSE.[32] The calculated defect levels are aligned with respect to the average electrostatic potential in Fig. 2(a). The defect levels are found at a nearly constant energy, independent of the adopted functional. This behavior results from the localized character of the defect wave function

TABLE III. Charge transition levels for the As antisite defect in GaAs as calculated with various functionals. The lattice constant ($a_0$) is fixed at the experimental value or determined consistently within the adopted theoretical scheme. The energies (in eV) are given with respect to the respective valence-band maxima. Experimental data are from Ref. 11.

| | Experimental $a_0$ | | Theoretical $a_0$ | |
|---|---|---|---|---|
| | +2/+1 | +1/0 | +2/+1 | +1/0 |
| PBE | −0.021 | 0.349 | −0.036 | 0.296 |
| HSE | 0.341 | 0.737 | 0.307 | 0.703 |
| PBE0 | 0.657 | 1.076 | 0.625 | 1.028 |
| tHSE | 0.507 | 0.916 | 0.567 | 0.972 |
| tPBE0 | 0.476 | 0.884 | 0.576 | 0.978 |
| Expt. | 0.54 | 0.77 | 0.54 | 0.77 |

and is consistent with previous studies.[1,5] In particular, we note that this behavior implies a small variation in the separation between the two defect levels. Indeed, the defect level separation can be expressed as $E^{0}_{\mathrm{tot}} - 2E^{+1}_{\mathrm{tot}} + E^{+2}_{\mathrm{tot}}$, which involves only total-energy differences corresponding to localized states. The calculated separation ranges between 0.37 and 0.42 eV, depending on the functional, in fair agreement with the experimental value of 0.23 eV.[11]

In Fig. 2(b), the same defect levels are aligned with respect to the valence-band maximum and their position in the band gap is compared to experimental levels. The numerical values are listed in Table III. We chose to compare our defect levels with those measured by Lagowski *et al.* at 0.54 and 0.77 eV.[11] Other measurements available in the literature differ by ∼20 meV,[10,12] which is consistent with the experimental accuracy. The PBE levels noticeably underestimate the experimental levels as a consequence of the severe band-gap underestimation. HSE gives a much better description of the band gap and the calculated +2/+1 and +1/0 levels are found within 0.2 and 0.05 eV from the measured levels, respectively. When the defect levels are given with respect to the conduction-band minimum, the errors are similar. In PBE0, the band gap is overestimated by ∼0.3 eV (Table I), leading to an overestimation of the defect levels by 0.1 and 0.3 eV when they are aligned with respect to the valence-band maximum. The agreement with experiment only slightly improves when the levels are referred to the conduction-band minimum.

To overcome ambiguities related to the band-gap error, we adjust the fraction $\alpha$ of nonlocal Fock exchange such that the theoretical band gap matches the experimental one. The defect levels calculated in such tuned HSE and tuned PBE0 schemes are very close to each other (Fig. 2). This is a consequence of the fact that when $\alpha$ is optimally tuned the band edges in tHSE and tPBE0 occur at the same energies with respect to the average electrostatic potential [cf. Fig. 2(a)].[5] This agreement is encouraging for the comparability between different kinds of hybrid functionals. Furthermore, the agreement with respect to experiment is very satisfactory, the calculated +1/0 and +2/+1 levels agreeing with the measured ones within only 0.15 and 0.06 eV, respectively.

We now consider the effects resulting from the lattice constant adopted for the GaAs host. In Fig. 3, the band edges

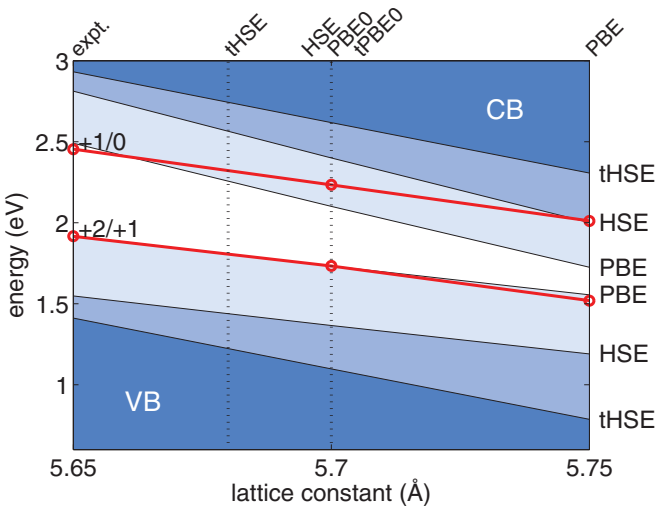


FIG. 3. (Color online) Band edges of GaAs aligned with respect to the average electrostatic potential as a function of lattice constant for various functionals. The defect levels of the unrelaxed As antisite are calculated with PBE, but their energies are also representative of the other functionals [cf. Fig. 2(a)]. The experimental and various theoretical lattice constants are indicated. The required fraction $\alpha$ of Fock exchange for tHSE increases from 0.34 to 0.53 as the lattice constant varies from 5.65 to 5.75 Å.

calculated with various functionals are shown as a function of the adopted lattice constant. The illustrated defect levels correspond to the unrelaxed As antisite. The defect energy levels are obtained with PBE but are only weakly dependent on the adopted functional [cf. Fig. 2(a)]. As the lattice constant increases beyond the experimental value (5.65 Å), the band gap reduces and both the band edges and the defect levels decrease with respect to the average electrostatic potential. When the hybrid functional is systematically tuned to match the experimental band gap, the required fraction of nonlocal Fock exchange increases with lattice constant. Within such a tuned scheme, the calculated defect levels shift to higher energies in the band gap as the lattice constant is increased (Fig. 3).

To examine the importance of this effect, we thus perform a second set of defect calculations, in which the lattice constant and the structural relaxations are consistent with the functional used. We adopt the theoretical lattice constant which generally overestimates the experimental one (Table I). The corresponding defect levels reported in Fig. 2(c) indicate that the changes associated to the lattice constant are minor. For tHSE and tPBE0, the deviation of the +1/0 level with respect to experiment increases to 0.21 eV, to be compared with the largest deviation of 0.15 eV for calculations at the experimental lattice constant. On the other hand, the +1/0 level now agrees within 0.04 eV.

It is interesting to study the nature of the defect wave functions, since the hybrid functionals tend to increase the localization of the wave functions due to reduction in the self-interaction. In Fig. 4(a), we show the density of the highest occupied defect orbital of the neutral As antisite in GaAs as calculated within the PBE. The density is illustrated through the superposition of two isosurfaces corresponding to high and

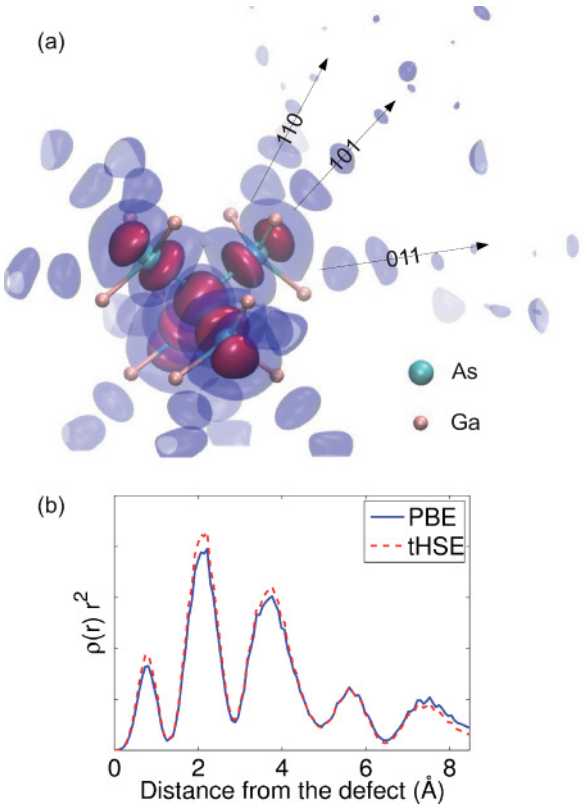


FIG. 4. (Color online) (a) Electron density of the defect state of the neutral As antisite in GaAs as calculated within the PBE. Two isosurfaces are superimposed, corresponding to high (opaque, red) and low (transparent, blue) values of charge density. (b) Comparison between the spherically integrated radial densities of the defect wave function as calculated in PBE (solid, blue) and in tHSE (dashed, red).

low charge densities. The charge density shows the tetrahedral symmetry and is mostly concentrated in the As-As bonds with tails extending in the (011) directions. In order to study the localization, we give in Fig. 4(b) the spherically integrated radial densities of the defect wave function as calculated in PBE and in tHSE. The wave function obtained within the hybrid functional scheme is indeed more localized, but the changes are minor. To give a quantitative description of the changes, we calculated the overlap between the wave functions obtained in the PBE and in the various hybrid functional schemes. As shown in Table IV, these overlaps are all very close to 1. This is consistent with previous calculations in the literature.[33]

## IV. CONCLUSIONS

For the As antisite, the present study indicates that tuned hybrid functional schemes yield defect level separations and defect level positions deviating from experiment by ∼0.2 eV. Our study also examines the effect of varying the bulk lattice constant in the defect calculations. We find that the energy

TABLE IV. Overlap between the defect wave functions of the neutral As antisite in GaAs as calculated with the PBE and with various other functionals.

| | HSE | PBE0 | tHSE | tPBE0 |
|---|---|---|---|---|
| Overlap with PBE | 0.993 | 0.991 | 0.989 | 0.994 |

levels of the As antisite defect shift by less than 0.1 eV when the lattice constant varies by ∼1%, corresponding to the difference between the theoretical and the experimental lattice constants in GaAs.

The separation between two charge transition levels is a property that derives solely from total-energy differences for localized states and does not involve the delocalized band-edge states. Insofar this condition applies, an analogy can be drawn with electron affinities and ionization potentials of molecular systems.[1,2] Hence, the achieved accuracy is expected to be similar to the overall accuracy with which hybrid functionals are able to reproduce such quantities, which is of the order of 0.2 eV.[34–36] The deviation of 0.19 eV from experiment found in this paper for the energy separation between the defect levels is thus fully consistent with these considerations and corresponds to the intrinsic accuracy of this class of functionals.

However, the defect energy levels as given with respect to the valence-band maximum also carry information about the energy position of delocalized band-edge states. To decouple the defect energy levels from the band-edge energies, it is convenient to refer both energies to the average electrostatic potential $\phi$.[1,2] Indeed, the energy levels of atomically localized defect states are generally well converged already within a semilocal density functional scheme when referred to $\phi$.[1,5] Hence, the comparison of the defect energy levels with experiment indicates that for GaAs the band-edge states referred to $\phi$ are also described within ∼0.2 eV. This overall accuracy for the determination of band edges with tuned hybrid functionals is consistent with calculated band offsets at a series of semiconductor-oxide interfaces.[5,37]

In conclusion, the errors observed in our study are consistent with the intrinsic accuracy of hybrid functionals both for the localized defect states and for the delocalized band-edge states. Hence, our results for the As antisite defect in GaAs support the notion that accurate defect levels can be achieved with hybrid functionals, provided the band gap and to a lesser extent the lattice constant of the host material are well reproduced.

## ACKNOWLEDGMENTS

Financial support is acknowledged from the Swiss National Science Foundation (Grants No. 200020-119733/1, No. 200020-134600, and No. 206021-128743). We used computational resources of CSCS and CSEA-EPFL.

[1] A. Alkauskas, P. Broqvist, and A. Pasquarello, Phys. Rev. Lett. **101**, 046405 (2008).
[2] A. Alkauskas, P. Broqvist, and A. Pasquarello, Phys. Status Solidi B **248**, 775 (2011).
[3] P. Mori-Sánchez, A. J. Cohen, and W. Yang, Phys. Rev. Lett. **100**, 146401 (2008).
[4] *Advanced Calculations for Defects in Materials: Electronic Structure Methods*, edited by A. Alkauskas, P. Deák, J. Neugebauer,

A. Pasquarello, and C. G. Van de Walle (Wiley-VCH, Weinheim, Germany, 2011).
[5]H.-P. Komsa, P. Broqvist, and A. Pasquarello, Phys. Rev. B **81**, 205118 (2010).
[6]J. Heyd, G. E. Scuseria, and M. Ernzerhof, J. Chem. Phys. **124**, 219906 (2006).
[7]P. Deák, B. Aradi, T. Frauenheim, E. Janzén, and A. Gali, Phys. Rev. B **81**, 153203 (2010).
[8]G. M. Martin and S. Makram-Ebeid, in *Deep Centers in Semiconductors*, edited by S. T. Pantelides (Gordon and Breach, New York, 1992).
[9]G. A. Baraff, in *Deep Centers in Semiconductors*, edited by S. T. Pantelides (Gordon and Breach, New York, 1992).
[10]E. R. Weber, H. Ennen, U. Kaufmann, J. Windscheif, J. Schneider, and T. Wosinski, J. Appl. Phys. **53**, 6140 (1982).
[11]J. Lagowski, D. G. Lin, T.-P. Chen, M. Skowronski, and H. C. Gatos, Appl. Phys. Lett. **47**, 929 (1985).
[12]P. Omling, P. Silverberg, and L. Samuelson, Phys. Rev. B **38**, 3606 (1988).
[13]R. M. Feenstra, J. M. Woodall, and G. D. Pettit, Phys. Rev. Lett. **71**, 1176 (1993).
[14]W. E. Spicer, I. Lindau, P. Skeath, C. Y. Su, and P. Chye, Phys. Rev. Lett. **44**, 420 (1980).
[15]W. E. Spicer, Z. Liliental-Weber, E. Weber, N. Newman, T. Kendelewicz, R. Cao, C. McCants, P. Mahowald, K. Miyano, and I. Lindau, J. Vac. Sci. Technol. B **6**, 1245 (1988).
[16]G. A. Baraff and M. Schlüter, Phys. Rev. Lett. **55**, 1327 (1985).
[17]J. Dabrowski and M. Scheffler, Phys. Rev. Lett. **60**, 2183 (1988).
[18]D. J. Chadi and K. J. Chang, Phys. Rev. Lett. **60**, 2187 (1988).
[19]S. B. Zhang and J. E. Northrup, Phys. Rev. Lett. **67**, 2339 (1991).
[20]J. T. Schick, C. G. Morgan, and P. Papoulias, Phys. Rev. B **66**, 195302 (2002).
[21]P. A. Schultz and O. A. von Lilienfield, Modell. Simul. Mater. Sci. Eng. **17**, 084007 (2009).
[22]J. P. Perdew, K. Burke, and M. Ernzerhof, Phys. Rev. Lett. **77**, 3865 (1996).
[23]J. P. Perdew, M. Ernzerhof, and K. Burke, J. Chem. Phys. **105**, 9982 (1996).
[24]M. Fuchs and M. Scheffler, Comput. Phys. Commun. **119**, 67 (1999).
[25]P. Broqvist, A. Alkauskas, and A. Pasquarello, Phys. Rev. B **80**, 085114 (2009).
[26]H.-V. Nguyen and S. de Gironcoli, Phys. Rev. B **79**, 205114 (2009).
[27]P. Giannozzi, S. Baroni, N. Bonini, M. Calandra, R. Car, C. Cavazzoni, D. Ceresoli, G. L. Chiarotti, M. Cococcioni, I. Dabo, A. Dal Corso, S. de Gironcoli, S. Fabris, G. Fratesi, R. Gebauer, U. Gerstmann, C. Gougoussis, A. Kokalj, M. Lazzeri, L. Martin-Samos, N. Marzari, F. Mauri, R. Mazzarello, S. Paolini, A. Pasquarello, L. Paulatto, C. Sbraccia, S. Scandolo, G. Sclauzero, A. P. Seitsonen, A. Smogunov, P. Umari, and R. M. Wentzcovitch, J. Phys. Condens. Matter **21**, 395502 (2009).
[28]A. Dal Corso and A. Mosca Conte, Phys. Rev. B **71**, 115106 (2005).
[29]J. S. Blakemore, J. Appl. Phys. **53**, R123 (1982).
[30]J. E. Peralta, J. Heyd, G. E. Scuseria, and R. L. Martin, Phys. Rev. B **74**, 073101 (2006).
[31]C. Freysoldt, J. Neugebauer, and C. G. Van de Walle, Phys. Rev. Lett. **102**, 016402 (2009).
[32]The choice of HSE is not critical, since the other functionals yield essentially the same relaxed defect geometry.
[33]A. Alkauskas and A. Pasquarello, Physica B **401**, 670 (2007).
[34]L. A. Curtiss, P. C. Redfern, K. Raghavachari, and J. A. Pople, J. Chem. Phys. **109**, 42 (1998).
[35]M. Ernzerhof and G. E. Scuseria, J. Chem. Phys. **110**, 5029 (1999).
[36]A. V. Krukau, O. A. Vydrov, A. F. Izmaylov, and G. E. Scuseria, J. Chem. Phys. **125**, 224106 (2006).
[37]A. Alkauskas, P. Broqvist, F. Devynck, and A. Pasquarello, Phys. Rev. Lett. **101**, 106802 (2008).